IJNAOE
©SNAK, 2014

Int. J. Nav. Archit. Ocean Eng. (2014) 6:935~946
http://dx.doi.org/10.2478/IJNAOE-2013-0223
pISSN: 2092-6782, eISSN: 2092-6790

Acoustic performance of industrial mufflers with CAE modeling and simulation

Soohong Jeon[1], Daehwan Kim[1], Chinsuk Hong[2] and Weuibong Jeong[3]

[1]*Graduate School of Mechanical Engineering, Pusan National University, Busan, Korea*
[2]*School of Mechanical Engineering, Ulsan College, Ulsan, Korea*
[3]*School of Mechanical Engineering, Pusan National University, Pusan, Korea*

ABSTRACT: *This paper investigates the noise transmission performance of industrial mufflers widely used in ships based on the CAE modeling and simulation. Since the industrial mufflers have very complicated internal structures, the conventional Transfer Matrix Method (TMM) is of limited use. The CAE modeling and simulation is therefore required to incorporate commercial softwares: CATIA for geometry modeling, MSC/PATRAN for FE meshing and LMS/ SYSNOISE for analysis. Main sources of difficulties in this study are led by complicated arrangement of reactive elements, perforated walls and absorption materials. The reactive elements and absorbent materials are modeled by applying boundary conditions given by impedance. The perforated walls are modeled by applying the transfer impedance on the duplicated node mesh. The CAE approach presented in this paper is verified by comparing with the theoretical solution of a concentric-tube resonator and is applied for industrial mufflers.*

KEY WORDS: Transmission loss; Industrial muffler; Transfer admittance; Acoustic finite element method; Acoustic performance.

INTRODUCTION

Mufflers are used in industrial application to reduce noise. They generally have reactive elements, perforated walls and absorbent materials. The reactive elements cause the transmission loss due to sudden expansion and contraction connected by extended inlet and outlet leading to the impedance mismatch. The perforated walls are also a sort of reactive elements producing the impedance mismatch. The absorbent materials on the other hand cause the transmission loss due to energy absorption while propagating sound wave.

There are several approaches to evaluate the transmission loss which are mainly based on the Transfer Matrix Method (TMM), the acoustic Finite Element Method (FEM), and the acoustic Boundary Element Method (BEM) (Bilawchuk and Fyfe, 2003). Munjal (1975) derived transfer matrices for various muffler elements with mean flow. Gerges et al. (2005) compared experimental results with the numerical predictions obtained from the TMM of the expansion chambers. However, the TMM can only be applied for simple mufflers with simple expansion chambers and concentric reactive elements. The conventional TMM to evaluate the transmission loss of industrial mufflers is hence of limited use because they have very complicated internal reactive structures. Dude and Sajanpawar (2007) investigated various mufflers having perforated walls and reactive

Corresponding author: *Chinsuk Hong*, e-mail: *cshong@uc.ac.kr*

elements using FEM. Soenark and Seybert (2000) examined a concentric tube resonator achieved with perforated walls using the multi-domain BEM. Ju and Lee (2005) calculated the transmission loss for the complicated three-dimensional silencers using the multi-domain BEM. CAE approaches based on FEM and BEM can be applied for the complicated industrial mufflers. However, the modeling of the complicated mufflers is not fully demonstrated yet.

In this paper, the modeling techniques for the reactive elements and the perforated wall of the industrial mufflers are demonstrated in detail using commercial software, MSC/PATRAN. The transmission loss of the muffler is then calculated using acoustic FEM capability of LMS/SYSNOISE.

INDUSTRIAL MUFFLER

Most of the industrial mufflers have reactive elements, perforated walls and absorbent materials to reduce the noise transmission. The reactive elements could be expansion and contraction, extended inlet and outlet, and various types of baffles. A typical industrial muffler thus can be represented as shown in Fig. 1. It has the extended inlet and outlet, perforated walls and three chambers separated by the baffles. The absorbent materials are imposed on the boundary of the industrial muffler.

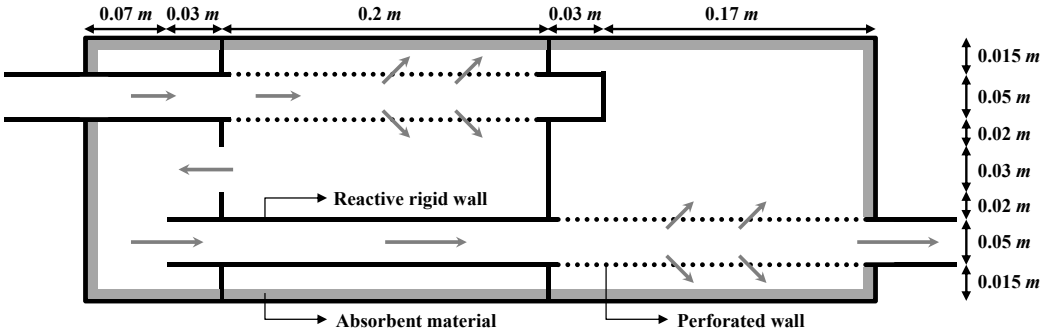

Fig. 1 Geometry and dimension of the industrial muffler.

The extended inlet and outlet and the baffles are reactive elements in this case. The perforated walls can be modeled as boundary conditions in CAE model. They can be modeled with boundary conditions in CAE model. The boundary conditions for the absorption materials are given by the surface impedance which can be either measured or calculated based on the two-microphone method as briefly explained in APPENDIX A. The absorption material in this case is glass wool. The boundary conditions for the reactive walls, which are in this case the extended inlet and outlet and baffles, are given by infinite impedance through the creation of the boundary face. The boundary conditions for the perforated walls can be defined by the transfer impedance. The transfer impedance can be evaluated using an experimental formula presented by Sullivan and Crocker (1978). This formula is based on the geometric parameters such as the porosity, thickness of the wall and the diameter of the holes. The perforated wall in this case has 10% of the porosity, 8 *mm* of the hole diameter and 2 *mm* of the thickness.

CAE MODELING

Absorbent materials

The absorbent material can be replaced by surface impedance, Z_a on the boundary of the industrial muffler using the two-microphone method that is demonstrated in APPENDIX A. The configuration of the numerical model is the same as that of the experimental model and the surface impedance for the absorbent material is computed by two-microphone method as in APPENDIX B. The absorbent material can then be replaced as the surface impedance. The validity of this approach is shown in APPENDIX B. It is assumed that the absorbent materials cover only the boundary of the industrial muffler as shown in Fig. 1. Thus, the surface impedance calculated by using two-microphone method can be simply imposed on the boundary of the industrial muffler. After the FE modeling process is done using PATRAN, the faces contacted with absorbent materials are selected in SYSNOISE. The surface impedance is then imposed on the selected faces.

Reactive elements

The reactive elements of the industrial mufflers are assumed to be rigid walls. This means that the reactive elements have acoustically infinite impedance. To give the infinite impedance boundary condition to the reactive rigid wall, the two faces are created in geometry modeling using CATIA. The distance between two faces is the same as the thickness of the reactive rigid wall. The face in the acoustic FEM has in default the infinite impedance. It means that it is not necessary to impose boundary condition to the face in a separate way. Thus, the reactive rigid wall is modeled by separated two faces as shown in Fig. 2. is noted that the nodes on the two faces are not necessary to match in this case for the rigid walls. The fluid domains separated by the reactive wall can make meshes independently.

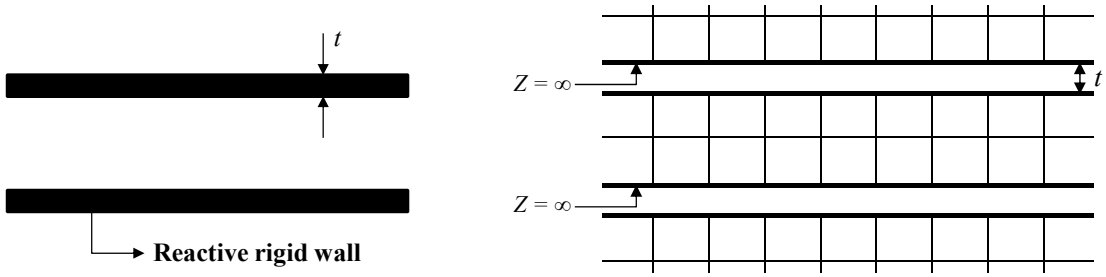

(a) (b)

Fig. 2 Reactive elements modeling: (a) geometry of reactive rigid wall; (b) infinite impedance boundary condition for the reactive elements.

Perforated walls

The perforated wall is modeled with two faces, as shown in Fig. 3, having the transfer admittance relation (LMS. SYSNOISE rev 5.6, 2003a):

$$\begin{bmatrix} v_{n1} \\ v_{n2} \end{bmatrix}_i = \begin{bmatrix} \beta & -\beta \\ -\beta & \beta \end{bmatrix}_i \begin{bmatrix} p_1 \\ p_2 \end{bmatrix}_i , \tag{1}$$

where v_{n1} and p_1 are the normal velocity and the pressure at a node on the first face, respectively, and v_{n2} and p_2 are those at the corresponding nodes on the second face. The transfer admittance denoted by β in Eq. (1) can be obtained by the transfer impedance given by Sullivan and Crocker (1978) for the case of zero mean flow, which depends on the hole size, porosity, wall thickness (Munjal, 1987). The resistance is constant for the linear case and approximated by R=2.4$kgm^{-2}s^{-1}$ and the reactance also can be approximated by $X=\rho ck(t+0.75d)$. The specific acoustical impedance is therefore written by Sullivan and Crocker (1978);

$$\zeta = \frac{1}{\rho c \sigma}(R + jX) = [6\times 10^{-3} + jk(t + 0.75d)]/\sigma , \tag{2}$$

where ρ is the density of the air, c is the speed of the sound, k is the wave number, t is the thickness of the wall, d is the hole size and σ is the porosity. Note that the transfer admittance is defined by;

$$Z_p = R + jX , \tag{3}$$

and it can also be expressed as the pressure difference Δp across the perforated wall divided by the average particle velocity v, i.e.,

$$Z_p = \Delta p / v . \tag{4}$$

The transfer admittance, β, can finally obtained as the inverse of Z_p:

$$\beta = 1/Z_p = 1/(\rho c \zeta) . \tag{5}$$

Now we demonstrate the modeling procedure while utilizing analysis software, e.g., LMS.SYSNOISE. To use the concept of the transfer admittance given by Eq. (5), the perforated surface should be modeled with two faces as mentioned above.

The two acoustic domains, connected each other through the perforation in practice, are first modeled with the two separate domains, and the perforated surfaces are then designated as the first face and the second faces as demonstrated in Fig. 3. The transfer admittance relation between the two faces is finally assigned. Assuming uniform perforation over the surface as shown in Fig. 3(a), the transfer admittance β can be given over the perforation. It is noted that the pair of the nodes on each face should be placed at the same span-wise location with the gap of the thickness of the surface in this case. Otherwise the model of the perforation works improperly, or includes a numerical fatal error. Using the node duplication process in LMS.SYSNOISE, the two faces can be created to impose the boundary condition of the perforated walls. Once the node duplication is done, the internal free faces are created as shown in Fig. 4. The free faces are then connected by the transfer admittance relation. Since the node duplication means a creation of new nodes at the same positions of the original nodes (LMS.SYSNOISE rev 5.6, 2003b), the node pairs on each face are automatically matched.

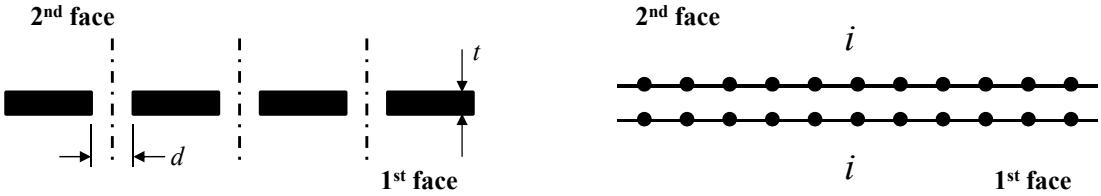

(a) (b)

Fig. 3 Modeling of a thin perforated wall with two faces having the transfer admittance relations.

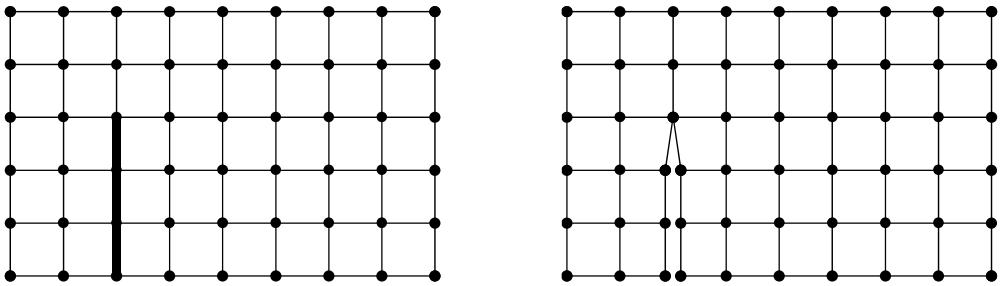

(a) (b)

Fig. 4 Node duplication: (a) original node selection for the duplication;
(b) result of node duplication (internal free face and two surfaces).

However, the node duplication process cannot be easily performed for three-dimensional problems due to the difficulties in selecting the internal nodes to duplicate. To solve those difficulties effectively for the three-dimensional complicated geometry, the following steps are suggested in this paper.

To match the node pairs on the two faces, the whole geometry of the industrial muffler firstly has to be grouped in one. Secondly, additional 2D elements are required to place on the two faces to effectively mat the nodes on the faces. Thirdly, 3D elements are then created based on the nodes of the 2D elements on the faces. After those processes, the 3D elements have to be renumbered for the face creation. From the renumbering process, the 3D element numbers can be known and identified. Finally,

SYSNOISE uses the identification numbers of the 2D elements to create the face. This process can be easily implemented in SYSNOISE using SYSNOISE Command Language (SCL).

The process of the node matching and renumbering are explained for a simple case of concentric quarter cylinders. The concentric quarter cylinders and groups are shown in Fig. 5(a). Grouping the two solids is done firstly to easily create quadrilateral 2D elements on the each face of the solid as shown in Fig. 5(b). FE meshing process for each solid is secondly done. After that, the tetrahedral 3D elements that have the same location of the nodes with that of the quadrilateral 2D elements are created as shown in Fig. 5(c). Before the acoustical analysis, the quadrilateral 2D elements have to be deleted. The solid elements with the face created by uniform surface elements can now be renumbered to create faces for the transfer impedance relation. The solid elements of inner quarter cylinder are renumbered from element number 1000 and those of outer are done from element number 2000. The FE model is imported in SYSNOISE and arbitrary face set is created. The set is extracted and written in SYSNOISE log file. In the log file, the face numbers which are required to know for the transfer impedance relation and element numbers which are renumbered by user are written subsequently, which is shown in Fig. 6(a). The element numbers are known value and then the face numbers can be known. The face numbers are written again as SCL as shown in Fig. 6(b). By reading SCL file, the face sets are obtained independently as shown in Fig. 7. Finally, the two faces are selected independently by SCL, and then connected by the transfer impedance relation.

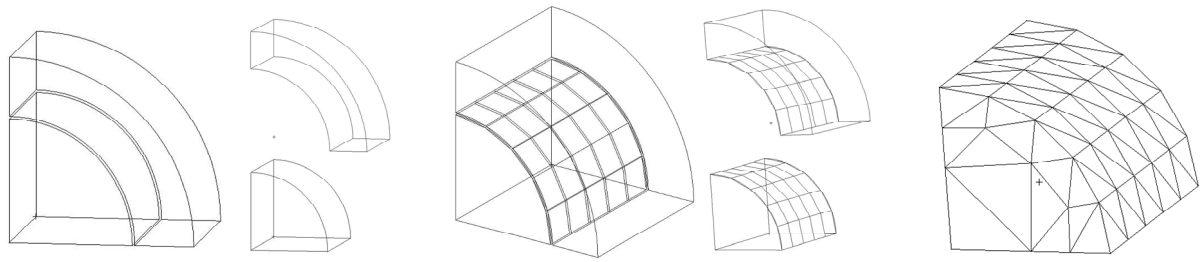

(a) (b) (c)

Fig. 5 Process of matching the nodes for the two faces to be connected with the transfer admittance relation: (a) geometry and groups of the inner and outer quarter cylinder; (b) quadrilateral 2D elements on the each face; (c) tetrahedral 3D elements that have same location of the nodes with that of quadrilateral elements 2D on the each face.

```
Face Elemt  Face Local
Numbr Numbr  Type Face# Nodes defining face topology
-------------------------------------------------------------------------------
 101  1005 TRIA3    4    2    3    9
 102  1006 TRIA3    3   15    9   16
 103  1007 TRIA3    2   14   15   21
 104  1008 TRIA3    3   20   14   21
 105  1009 TRIA3    3    8    9   15
```

(a)

```
Set 1 name 'inner'
Faces 101 102 103 104 105 106 107 108 109 110
Faces 111 113 114 115 117 119 120 121 122 123
Faces 124 125 126 128 130 131 132 137 141 143
Faces 144 145 146 148 149 153 157 161 162 163
Faces 164 165 171 175 179 181 183
Return
```

(b)

Fig. 6 (a) SYSNOISE log file that contains the arbitrary face numbers and element numbers; (b) SCL that can allow user to obtain the face selections.

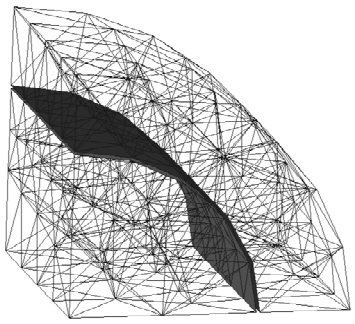

Fig. 7 Two faces defined by using SYSNOISE command language.

SIMULATION

Concentric-tube resonator model

For the comparison with the numerical and experimental results of Sullivan and Crocker (1978), the test model of concentric-tube resonator is considered before the simulation of the industrial muffler shown in Fig. 1. The dimension of the test model is shown in Fig. 8(a) and the FE model for the analysis for the comparison is shown in Fig. 8(b). The flow rate of this analysis is zero. The muffler is modeled by two domains of FE model for the modeling of the perforated wall as demonstrated in CAE MODELING section. The hole diameter of the perforated wall is 2.49 *mm* and the thickness of the perforated wall is 0.81 *mm*. The porosity of the perforated wall is 3.8%. From the porosity and the dimension of the concentric-tube resonator, the transfer admittance matrix is computed.

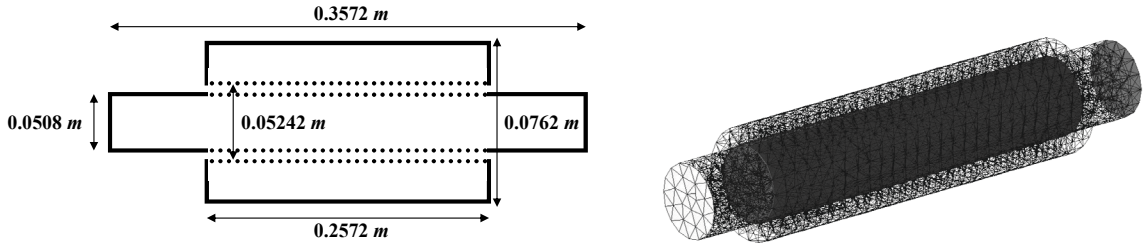

(a) (b)

Fig. 8 Concentric-tube resonator: (a) geometry of the concentric-tube resonator; (b) acoustical model for the analysis.

In the acoustic FEM, following equation for the harmonic analysis is used to solve the pressures p (Munjal, 1987).

$$\left([M]-k_0^2[K]+j\rho_0\omega[C]\right)\{p\}=-j\omega\rho_0\{F\}, \tag{6}$$

where $[M]$ is the mass matrix, $[K]$ is the stiffness matrix, $[C]$ is the damping matrix, $\{F\}$ is the force vector, k_0 is the wave number, and ρ_0 is the density of the air.

For the calculation of the transmission loss, the boundary conditions are imposed at the inlet and outlet. The Normal velocity with the harmonic amplitude 1 *m/s* is given to the inlet. The impedance for the non-reflecting boundary is given to the outlet. The impedance of the outlet is same as that of the air.

The transmission loss of Sullivan and Crocker (1978) for the concentric-tube resonator is shown in Fig. 9(a) and that of acoustic test model is shown in Fig. 9(b). The transmission loss of the concentric-tube resonator has a good agreement with Sullivan and Croker's results as shown Fig. 9.

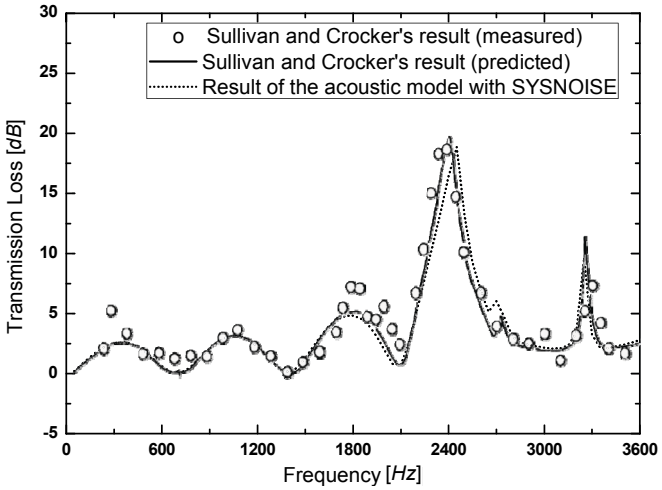

Fig. 9 Transmission loss for the concentric-tube resonator without a mean flow (——— Sullivan and Crocker's predicted result, o Sullivan and Crocker's measured result, - - - - - - Numerical analysis result with SYSNOISE).

The absorbent materials demonstrated in CAE MODELING section is attached at the inside wall of the outer tube as shown in Fig. 10(a). The thickness of the absorbent material used for this model is 0.01 *m*. The surface impedance is calculated using numerical two-microphone method shown in Fig. 16. This analysis has no mean flow. Fig. 19 shows (a) the sound absorption coefficient and (b) the acoustic impedance estimated by the numerical two microphone method. In SYSNOISE, the surface impedance is used for the boundary condition of the absorbent wall of the muffler as shown in Fig. 10(b). Fig. 11 shows the transmission loss of the concentric-tube resonator with the absorbent material. It follows that the absorbent material leads to a higher transmission loss and a slight shift to lower frequencies. The CAE modeling processes are therefore validated to apply for the industrial muffler with absorbent materials, reactive elements and perforated walls.

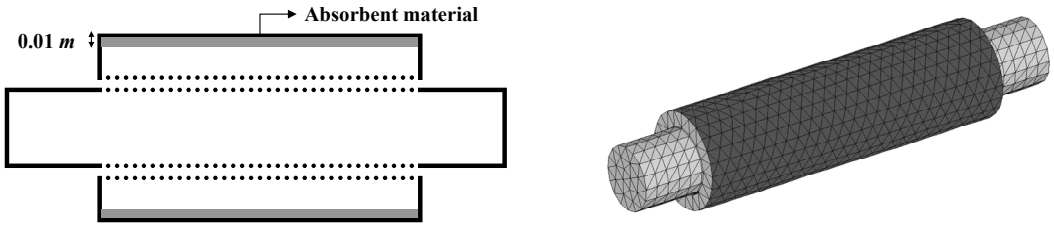

(a) (b)

Fig. 10 (a) Concentric-tube resonator that has absorbent material at the boundary; (b) surface impedance boundary condition.

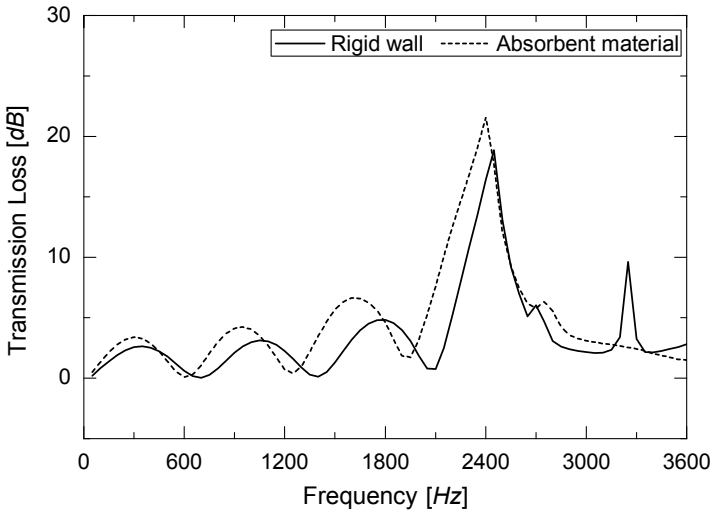

Fig. 11 Transmission loss of the concentric-tube resonator covered with absorbent materials.

Industrial muffler model

Industrial muffler model for the analysis is shown in Fig. 12. The selected faces for the transfer impedance relations are shown in Fig. 12(a). The perforated walls are modeled as shown in Fig. 1. The surface impedance boundary condition is imposed on the boundary of the muffler as demonstrated in INDUSTRIAL MUFFLER section.

The maximum length of elements for the industrial muffler model is 0.01 *m*. The reliable frequency range is calculated by the following equation (LMS.SYSNOISE rev 5.6, 2003c).

$$f_{\max} \le \frac{c}{6 \cdot l_{\max}}, \tag{7}$$

where $f_{\max}$ is the maximum frequency for the reasonable accuracy, c is the sound speed, and $l_{\max}$ is the maximum length of elements. The maximum frequency of the industrial muffler model is 5,667 *Hz* and mesh size of this model is reasonable.

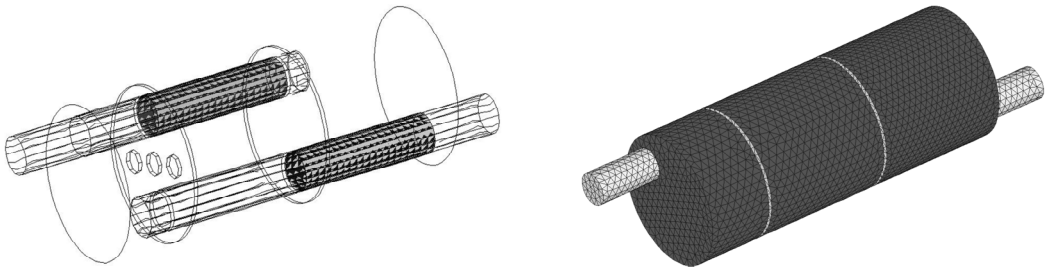

(a) (b)

Fig. 12 Industrial muffler model: (a) selected faces for the transfer admittance relations; (b) boundary for the surface impedance boundary condition corresponding to absorbent materials.

For the evaluation of convergence of the element size, the industrial muffler model used in this paper is compared with another model having the element size 0.005 *m* as shown in Fig. 13. In this comparison, the absorbent material is not considered. From the comparison of the transmission loss, the results of two cases have good agreement. It shows that used element size is recommendable. With the surface impedance boundary conditions, the transmission loss of the industrial muffler is calculated for the two cases. The absorbent material is not considered in the first case. In the second case, the absorbent material is considered. The transmission losses for the two cases are shown in Fig. 14.

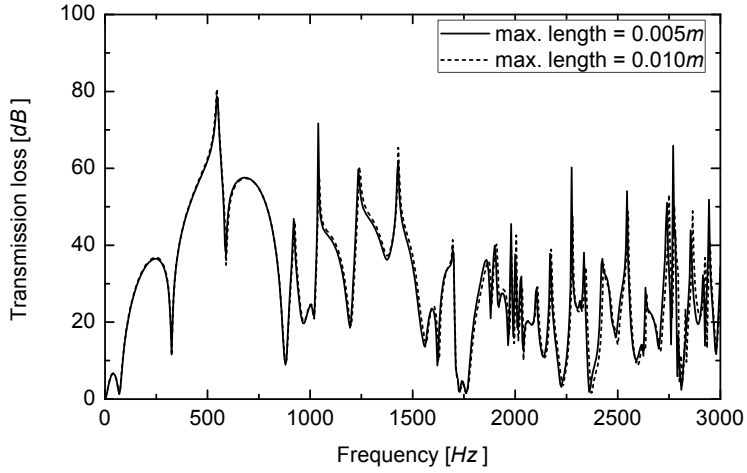

Fig. 13 Transmission loss of the industrial muffler
(——— maximum length of elements is 0.005 *m*, - - - - - - maximum length of elements is 0.010 *m*).

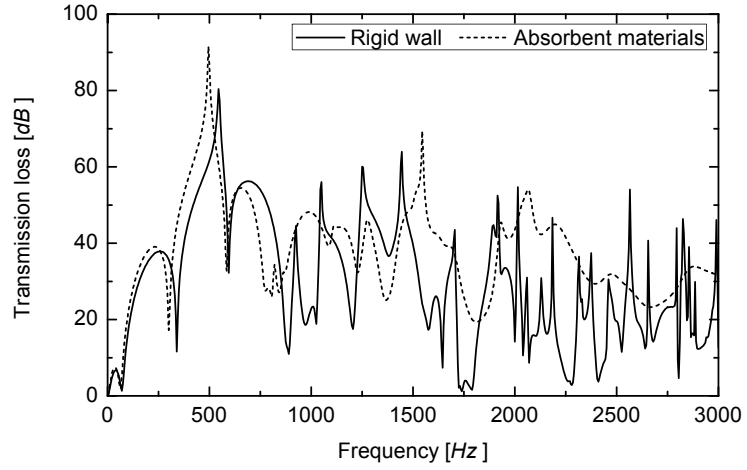

Fig. 14 Transmission loss of the industrial muffler
(——— rigid wall boundary condition, - - - - - - impedance boundary condition imposed the absorbent materials).

The transmission loss of the industrial muffler without absorbent material is denoted by the solid line in Fig. 14. In the result, the transmission loss has a high level because of the partitioned chambers and the perforated walls. There is a dominant peak at 500 *Hz* and higher-order acoustic mode is appeared above the frequency of the peak. It shows the reasonable features in the transmission loss of industrial mufflers having chambers and perforated walls. The dotted line in Fig. 14 shows the transmission loss of the industrial muffler with absorbent materials. When absorbent materials are applied to the industrial muffler, the transmission loss is increased and the spectrum is shifted to lower frequencies.

CONCLUSIONS

The technique of modeling the absorbent materials, the reactive elements and the perforated walls has been established and then applied for industrial mufflers. The absorbent materials were modeled as the impedance boundary condition given by the numerical two-microphone method. The calculated surface impedance was imposed on the absorbent boundary of the industrial muffler. The reactive elements were assumed to be rigid walls and imposed with the infinite impedance. The perforated walls were modeled using the transfer admittance relation. SYSNOISE log file and SCL file were used for automatically creating the transfer admittance relation. To verify the established numerical modeling process, the simulation was performed for the concentric-tube resonator of which measured transmission loss is available. The transmission losses of the numerical and experimental results were fairly well matched. Based on these processes, the complex industrial muffler can be modeled and the acoustic performance can be predicted more effectively.

REFERENCES

ASTM International, 1998. *ASTM E1050 Standard test method for impedance and absorption of acoustical materials using a tube, two microphones, and a digital frequency analysis system*. West Conshohocken: ASTM International.

Bilawchuk, S. and Fyfe, K.R., 2003. Comparison and implementation of the various numerical methods used for calculating transmission loss in silencer system. *Applied Acoustics*, 64(9), pp.903-916.

Dude, P. and Sajanpawar, P.R., 2007. Study of perforated mufflers of circular and elliptic cross sections using parametric technique and finite element methodology. *SAE paper, 2007-01-0895*. Society of Automotive Engineers inc.: SAE International.

Gerges, S.N.Y., Jordan, R., Thieme, F.A., Bento Coelho, J.L. and Arenas, J.P., 2005. Muffler modeling by transfer matrix method and experimental verification. *Journal of the Brazilian Society of Mechanical Sciences and Engineering,* 27(2), pp.132-140.

Ju, H.D. and Lee, S.B., 2005. Transmission loss estimation of three dimensional silencers with perforated internal structures using multi-domain BEM. *Journal of Mechanical Science and Technology*, 19(8), pp.1568-1575.

LMS.SYSNOISE rev 5.6, 2003a. *User manual: model data*. Belgium: LMS International NV.

LMS.SYSNOISE rev 5.6, 2003b. *User manual: geometry modeling*. Belgium: LMS International NV.

LMS.SYSNOISE rev 5.6, 2003c. *User manual: extracting information*. Belgium: LMS International NV.

Munjal, M.L., 1975. Velocity ratio-cum-transfer matrix method for the evaluation of a muffler with mean flow. *Journal of Sound and Vibration*, 39(1), pp.105-119.

Munjal, M. L., 1987. *Acoustics of ducts and mufflers*. New York: John Wiley & Sons.

Schultz, T., Cattafesta, L. and Sheplak, M., 2006. Comparison of the two-microphone method and the modal decomposition method for acoustic impedance testing. *Proceedings of the 12th AIAA/CEAS Aeroacoustics Conference*, Cambridge, Massachusetts, 8-10 May 2006, pp.3826-3838.

Soenark, B. and Seybert, A.F., 2000. Visualization of wave propagation in muffler. *Journal of Visualization*, 3(3), pp.229-235.

Sullivan, J.W. and Crocker, M.J., 1978. Analysis of concentric-tube resonator having unpartitioned cavities. *The Journal of the Acoustical Society of America*, 64(1), pp.207-215.

APPENDIX A – Experimental two-microphone method

For measuring the impedance of an absorbent material, two-microphone method can be used. The experimental setup for the two-microphone method is shown in Fig. 15.

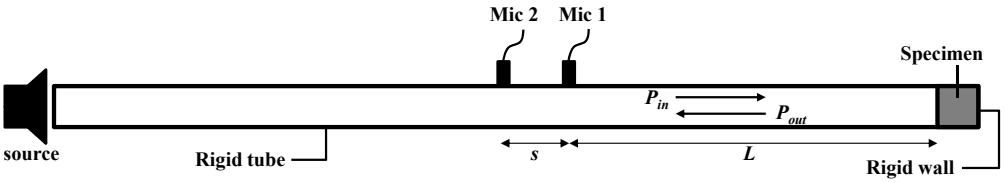

Fig. 15 Experimental set up for two-microphone method.

The acoustic transfer function of the two microphone signals can be derived as follows;

$$H_{12} = \frac{G_{12}}{G_{11}\overline{H}_c}, \tag{8}$$

where G_{12} is the cross power spectrum, G_{11} is the input auto power spectrum and $\overline{H}_c$ is the calibration factor. From the transfer function H_{12}, the pressure reflection coefficient R of the absorbent material is determined from the following equation;

$$R = \frac{H_{12} - e^{-jks}}{e^{jks} - H_{12}} e^{j2k(s+L)}, \tag{9}$$

where L is the distance from the specimen face to the first microphone and s is the distance between the two microphones. $k=2\pi f/c$, f is the frequency and c is speed of sound. From the reflection coefficient, the absorption coefficient α and impedance, $Z/\rho c$ of the specimen is determined (ASTM E International, 1998; Schultz et al., 2006).

$$\alpha = 1 - |R|^2, \quad \frac{Z}{\rho c} = \frac{1+R}{1-R} \tag{10}$$

APPENDIX B – Numerical two-microphone method

Using two-microphone method in an impedance tube, the acoustical performance of the absorbent material is numerically modeled as impedance boundary condition that depends on frequencies. The numerical impedance tube model is set up similar to the experimental one as shown Fig. 16. The diameter of the impedance tube is 0.02 *m*, the distance between two field points 0.01 *m* and the distance between from the absorbent material 0.5 *m*. The thickness of the absorbent material, glass wool in this case, at the end of the impedance tube is 0.01 *m*. The absorbent material has 96% of the porosity, 40,000 $Pa.s/m^2$ of the resistivity and 1.0 of the structural factor. The flow rate was set to zero.

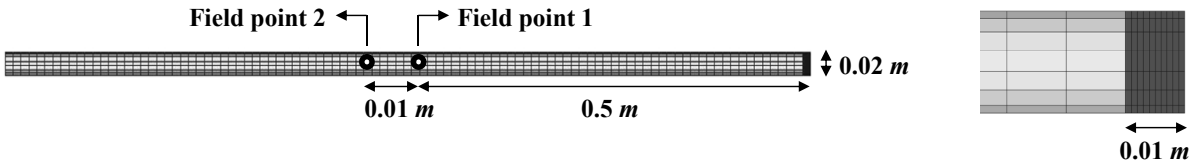

Fig. 16 Numerical model for the two-microphone method.

From the numerical model for the two-microphone method, the surface impedance Z_a is calculated and stored to the table. The surface impedance table is applied to the impedance boundary condition in SYSNOISE. To verify the reliance for applying absorbent material as surface impedance boundary condition, two cases are considered as shown Fig. 17.

The first case is that the absorbent material is located at the end of the tube as shown in Fig. 17(a) and second case is that the impedance boundary condition computed by the two-microphone method is imposed at the end of the tube as shown in Fig. 17(b). It is illustrated in Fig. 18 that the sound pressure of the two cases at same location of the each field point for the two cases. Fig. 18 shows the comparisons of (a) the real parts and (b) the imaginary parts of the sound pressure for the two cases. The results of comparison for the two cases are reasonable to apply the absorbent material as impedance boundary condition.

Characteristics of the absorbent material are shown in Fig. 19 that is calculated using the two-microphone method. The sound absorption coefficient and the specific acoustic impedance are shown in Figs. 19(a) and 19(b).

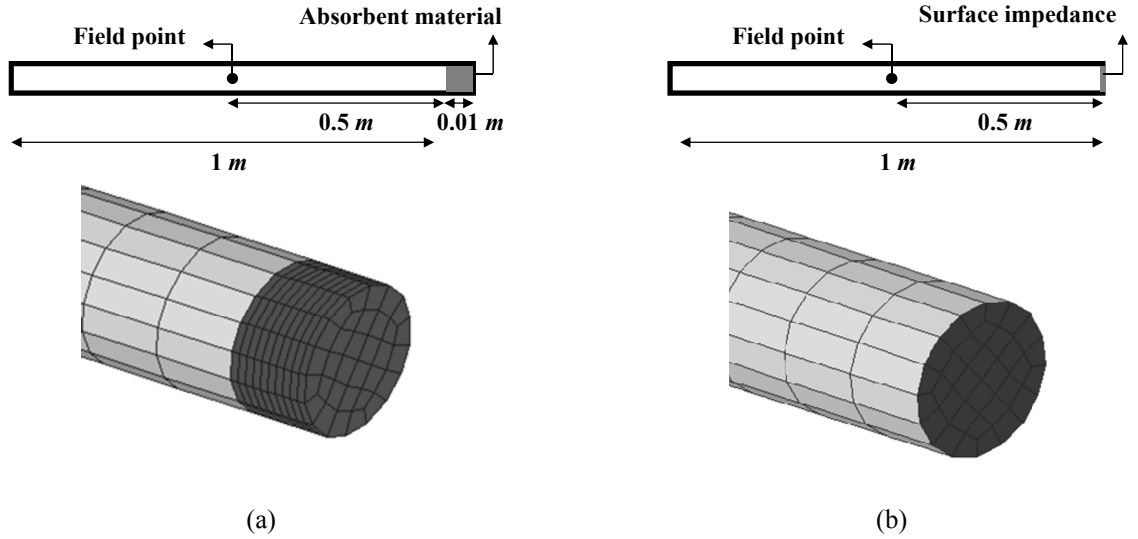

(a) (b)

Fig. 17 Boundary condition at the end of the tube: (a) absorbent material at the end of the tube; (b) surface impedance computed using two-microphone method at the end of the tube.

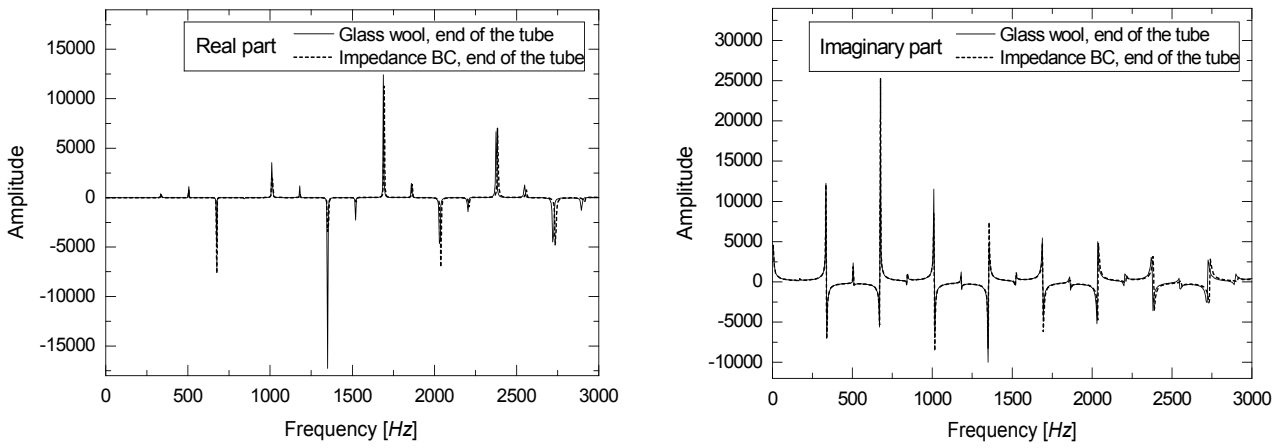

(a) (b)

Fig. 18 Comparison of the sound pressure at the center of in the tube with the absorbent material to that with the impedance boundary condition at the end of the tube: (a) real part of the sound pressure; (b) imaginary part of the sound pressure.

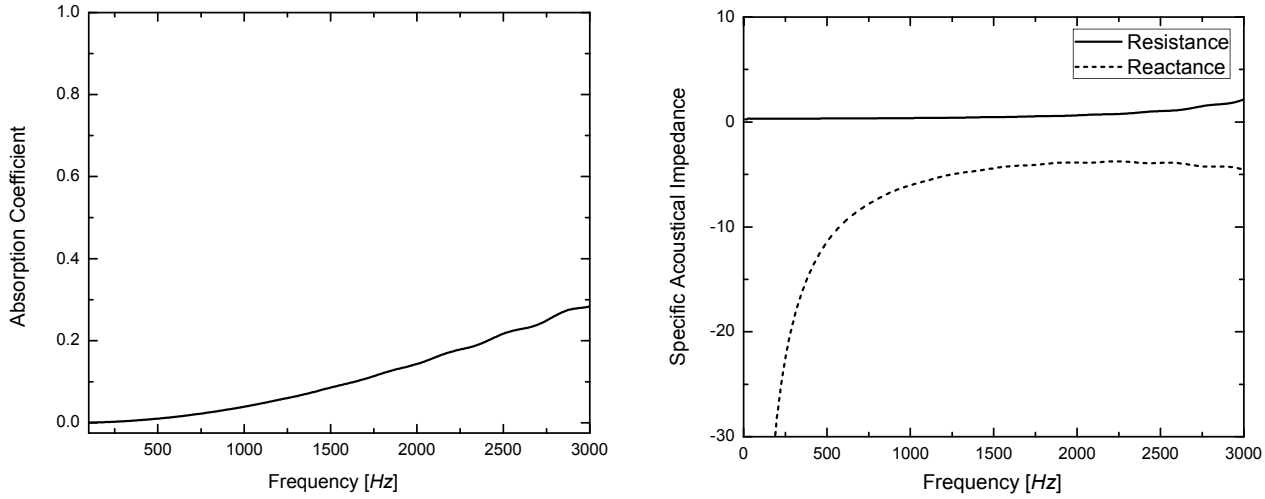

(a) (b)

Fig. 19 Characteristics of the absorbent material:
(a) sound absorption coefficient; (b) specific acoustical impedance.